Scripta Materialia 124 (2016) 51–55

Contents lists available at ScienceDirect

Scripta Materialia

journal homepage: www.elsevier.com/locate/scriptamat

Regular Article

Effect of strain hardening and volume fraction of crystalline phase on strength and ductility of bulk metallic glass composites

Mayuresh K. Shete [a], I. Singh [a], R. Narasimhan [a,*], U. Ramamurty [b]

[a] Department of Mechanical Engineering, Indian Institute of Science, Bangalore 560012, India
[b] Department of Materials Engineering, Indian Institute of Science, Bangalore 560012, India

ARTICLE INFO

Article history:
Received 29 April 2016
Received in revised form 15 June 2016
Accepted 19 June 2016
Available online xxxx

Keywords:
Metallic glass
Composites
Ductility
Strain hardening
Finite element analysis

ABSTRACT

Continuum finite element analyses are performed to ascertain the role played by the volume fraction (V_f) and strain hardening behavior of crystalline reinforcements on the strength and ductility of bulk metallic glass matrix composites (BMGCs). Results show that a highly strain hardening elongated dendrite with V_f ~45% would make the BMGC ductile without any penalty on the strength. These results provide design guidelines for strong yet ductile BMGCs.

© 2016 Elsevier Ltd. All rights reserved.

The proverbial 'Achilles heel' that is preventing widespread deployment of bulk metallic glasses (BMGs) in structural components is the lack of tensile ductility. This is due to localization of plastic flow into narrow regions that are often referred to as shear bands (SBs) [1–2]. Numerous materials engineering strategies are being pursued to circumvent this problem [2]. Amongst these, the composites approach, wherein a secondary crystalline dendritic phase is introduced into the microstructure, is most promising. While the dendritic phase imparts the required ductility, a concomitant reduction in strength, by virtue of the fact that its yield strength is much lower than that of the bulk metallic glass (BMG) matrix, is inevitable [2–5]. While several experimental and few modeling studies on these composites have been already reported in literature [3–10], many questions remain unanswered. For example, 'What is the optimum combination of microstructural and material parameters such as volume fraction (V_f), size, morphology and strain hardening behavior of the dendrites, and the inter-dendritic spacing that would give high ductility without compromising on the strength of BMG?' To address this issue, detailed continuum simulations can be useful, since an experimental study, wherein only one of the aforementioned microstructural parameters is varied while keeping others constant, is difficult. Hence, we have performed finite element simulations of tensile deformation response of BMGCs wherein both V_f and strain hardening exponent, N, are varied systematically.

Fig. 1 shows a plane strain tension specimen discretized into 5760 four-noded quadrilateral elements. The top edge of this specimen is stretched at a constant strain rate of $2 \times 10^{-3}\ s^{-1}$, while the bottom edge is restrained from moving in X_2 direction. Motivated by the fine and elongated dendrites observed in microstructures of various BMGCs [10–12], the dendrites are assumed to have rounded-rectangular shape with an aspect ratio of four, and dispersed uniformly in the BMG matrix. Three values of V_f (17%, 30% and 45%) are considered. While more complex BMGC microstructures could be modeled, they will not yield clear insights about how V_f and N influence the mechanism of plastic deformation and failure under tensile loading.

A thermodynamically consistent, finite deformation, non-local plasticity theory [13], which has been shown to predict the mechanical behavior of BMGs [13–16] and nanoglasses [17] well, is employed to represent the constitutive response of the BMG matrix. The use of such a model ensures accurate representation of shear localization, an important attribute of plastic deformation in BMGs, without being sensitive to the mesh [18]. This is accomplished by making the size of elements much smaller than the expected SB width, which scales with the internal material length, l_c, in the model (see below) [16,17]. The evolution of free volume, ξ, is governed by diffusion, creation by plastic shearing and hydrostatic stress, and annihilation by structural relaxation as [13]:

$$\dot{\xi} = \dot{\xi}_o(s_1/s_3)\left(\nabla^2\xi\right) + \zeta\dot{\gamma} - \left(\dot{\xi}_o\overline{p}/s_3\right) - \dot{\xi}_o(s_2/s_3)(\xi - \xi_T). \quad (1)$$

* Corresponding author.
E-mail address: narasi@mecheng.iisc.ernet.in (R. Narasimhan).

http://dx.doi.org/10.1016/j.scriptamat.2016.06.020
1359-6462/© 2016 Elsevier Ltd. All rights reserved.

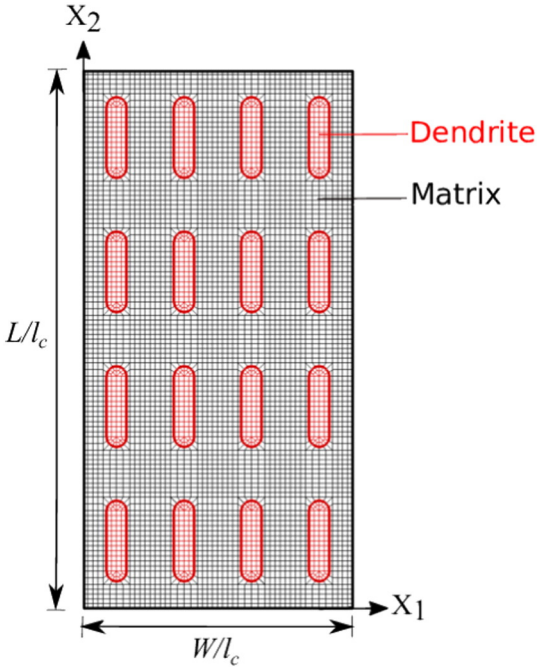

Fig. 1. Finite element model employed in plane strain tension simulation of BMGCs consisting of dendrites uniformly distributed in BMG matrix ($V_f = 17\%$). The normalized dimensions of the specimen are 40 (W/l_c) × 80 (L/l_c).

Here, $\dot{\xi}_o = f_o \exp(-\phi/2\xi)$, where f_o is a reference frequency and ϕ a geometrical factor. Also, s_1 and s_2 are gradient and defect free energy coefficients (with units of energy per unit length and volume, respectively), while s_3 controls the resistance to free volume generation. Further, ζ is coefficient of free volume generation due to plastic shearing, $\overline{p}$ hydrostatic pressure, ξ_T the fully annealed free volume at temperature T [13].

Also in Eq. (1), $\dot{\gamma}$ is the rate of plastic shearing which is given by:

$$\dot{\gamma} = \begin{cases} \dot{\gamma}_o \left(\frac{f^p}{c}\right)^{\frac{1}{a}} & \left(f^p = \overline{\tau} - \zeta\left(-s_1\left(\nabla^2\xi\right) + s_2(\xi - \xi_T) + \overline{p}\right) > 0\right), \\ 0 & (f^p \le 0). \end{cases} \quad (2)$$

Here, $\dot{\gamma}_o$ is the reference shear strain rate and $a > 0$ strain rate sensitivity parameter. Further, $\overline{\tau}$ is the Mises shear equivalent stress, while rest of the terms in f^p constitute a back stress [13,16,17] and c is cohesion. It is assumed to evolve as $c = c_o \exp\{-k(\xi - \xi_T)\}$, where c_o is the initial value and $k < 0$, a constant that controls free volume induced softening. The initial cohesion is slightly perturbed (by 1%) following a normal distribution and randomly assigned to the BMG matrix in order to trigger SBs [16,17]. Most of the material parameters in the plasticity model are taken from the work of Thamburaja [13] which are typical of BMGs. The ratio of Young's modulus to initial mean cohesion, E/c_o and Poisson's ratio are chosen as 100 and 0.38, respectively. The parameter ζ is taken as 0.02, ξ_T as 0.00063 at $T = 293$ K, s_2/c_0 as 2800 and s_3/c_0 as 240. The constants f_o, ϕ, k, $\dot{\gamma}_o$ and a are assumed as 323 s^{-1}, 0.15, -250, 1.73×10^{-3} s^{-1} and 0.02, respectively. It can be seen from Eq. (2) that a material length, l_c enters into the model through constant s_1, which is taken as $l_c = \sqrt{s_1/s_2}$ [16,17]. All geometrical lengths in this work are normalized by l_c.

The crystalline phase is assumed to follow J_2 flow theory of plasticity with power law hardening of the form:

$$\frac{\overline{\varepsilon}^p}{\varepsilon_y} = \left(\frac{\overline{\sigma}}{\sigma_y}\right)^{\frac{1}{N}} - 1, \quad \overline{\sigma} \ge \sigma_y. \quad (3)$$

Here, $\overline{\sigma}$ and $\overline{\varepsilon}^p$ are Mises tensile equivalent stress and plastic strain, respectively. Also, σ_y and ε_y are the initial tensile yield stress and strain, respectively. While the Young's modulus of dendrites is taken to be 50% higher than the matrix [5,7,19], σ_y is assumed to be 40% lower [3–5]. Three values of N (0.1, 0.2 and 0.3) are considered.

Normalized nominal stress (Σ_2/c_o) versus nominal strain (E_2) curves of the monolithic BMG and BMGCs with different V_f and $N = 0.2$, are displayed in Fig. 2(a). The responses of the BMGCs deviate from linearity at $E_2 \sim 0.01$–0.015. Thereafter, stress continues to increases till it reaches a peak, $\hat{\Sigma}$. It is lower for BMGCs than the monolithic BMG and reduces further with increase in V_f, while the corresponding E_2 increases. This can be rationalized by noting that $\hat{\Sigma}$ is mainly governed by the yield strength of the matrix and average stress in dendrites at onset of global yielding in the composite. Interestingly, while curves pertaining to lower V_f attain the peak immediately after deviating from the linear regime, the $V_f = 45\%$ case exhibits perceptible strain hardening before $\hat{\Sigma}$ is reached. Although similar trends have been observed in experiments on BMGCs [5,11,20,21], the mechanistic origin for the strain hardening is not well understood. The present simulations show that the slope of the stress-strain curve, $d\Sigma_2/dE_2$, for BMGC follows the rule of mixture in the range of E_2 from 0.02 to 0.024 and becomes positive for high $V_f = 45\%$ (Fig. 2(b)). This implies that *competition between free volume induced softening in the matrix and hardening in dendrites governs macroscopic strain hardening observed in BMGCs.*

Further, in the case of BMG, an abrupt drop in stress occurs at $E_2 \sim 0.025$ signifying rapid strain localization in the dominant SB [13,16,17]. A similar, but less steep, stress drop takes place in BMGC with $V_f = 17\%$ at a higher strain. With increase in V_f, the abrupt stress drop gets further delayed and becomes more gradual. Finally, when $V_f = 45\%$, the BMGC shows no sharp stress drop up to $E_2 = 0.1$. *These results clearly show that an increase in V_f delays the process of flow localization and also tends to stabilize it as evidenced by accompanying stress drop becoming less steep.*

Further insights into the flow mechanism are obtained through contour plots of maximum principal logarithmic plastic strain log λ_1^p which are displayed in Figs. 3 and 4. Fig. 3(a) shows that a mature SB with large plastic strain has formed in the BMG at $E_2 = 0.025$ leading to rapid softening induced by free volume evolution (see Eq. (1)) and steep drop in stress. By contrast, dendrites in BMGC begin to yield earlier owing to their low σ_y (Fig. 3(b) and (e)). This, in turn, leads to a strain mismatch at matrix-dendrite interfaces and large stress concentration within the matrix separating two adjacent rows of dendrites. Consequently, these regions act as SB nucleation sites where plastic yielding initiates (Fig. 3(b)). On subsequent loading, while plastic deformation remains homogeneous within the dendrites, it begins to localize in the matrix for $V_f = 30\%$ (Fig. 3(c)) causing rapid stress drop at $E_2 = 0.03$–0.04 (Fig. 2(a)). However, the dendrites in the path of the dominant SB hinder its propagation (see dendrites 'a' and 'b' in Fig. 3(c)). When E_2 is increased to 0.06, the SB penetrates through the above dendrites as well and spans the entire specimen width leading to shear offset m-m (Fig. 3(d)). A second dominant SB in the specimen's lower-half, which is blocked by dendrites 'c' and 'd', localized neck n-n, as well as numerous weak secondary SBs indicated by arrows, may also be seen in Fig. 3(d).

On comparing Fig. 3(e) with (b), it is observed that the number of SB nucleation sites in the matrix is more for $V_f = 45\%$. However the inter-dendritic spacing gets reduced, which makes localization difficult due to non-availability of straight paths for unhindered shear band propagation. Overall, this leads to multiple SBs within the sample, and more uniformly distributed plastic strain, see Fig. 3(f), (g), except for some inter-dendritic regions near the specimen sides where localized necks have developed (Fig. 3(g)). Consequently, the macroscopic stress drops gradually with strain for this case (Fig. 2(a)). However, when E_2 is increased to 0.1, two dominant SBs extend across the specimen, penetrating and distorting some dendrites while circumventing a few others (see arrows in Fig. 3(h)). The localized necks indicated by m-m and n-n also become more pronounced at this stage. Thus the deformation mechanism seen

Download English Version:

https://daneshyari.com/en/article/7911467

Download Persian Version:

https://daneshyari.com/article/7911467

Daneshyari.com